THE ASTROPHYSICAL JOURNAL, 455:75–87, 1995 December 10

THE CANADA-FRANCE REDSHIFT SURVEY. III. "SINGLE EMISSION-LINE" OBJECTS, ANALYSIS OF REPEAT OBSERVATIONS, AND SPECTROSCOPIC IDENTIFICATIONS IN THE 1415+52 AND 2215+00 FIELDS

S. J. LILLY[1]
Department of Astronomy, University of Toronto, Toronto, Ontario, Canada M5S 1A7
F. HAMMER[1] AND O. LE FÈVRE[1]
DAEC, Observatoire de Paris–Meudon, 92195 Meudon, France
AND
DAVID CRAMPTON[1]
Dominion Astrophysical Observatory, Victoria, British Columbia, Canada V8X 4MC
Received 1994 December 27; accepted 1995 June 19

ABSTRACT

This paper is one of a series describing the Canada-France Redshift Survey (CFRS). It is shown how the shape of the continuum around the emission line can be used to distinguish between [O II] λ3727 at $z > 0.76$ and Hα at low redshift in spectra for which only a single isolated emission line is visible. Based on this, [O II] λ3727 is most likely to be the emission line in most of the single emission-line galaxies in the CFRS. The statistics of the repeated observations are analyzed to derive an empirical calibration of the reliability of the spectroscopic identifications in the CFRS in order to determine how often additional observations could lead to the identification of an initially unidentified object and to provide an estimate of the internal velocity accuracy. Finally, the results of spectroscopic observations of 413 objects in the 1415+52 and 2215+00 CFRS survey fields are presented.

Subject headings: catalogs — galaxies: distances and redshifts — line: identification

1. INTRODUCTION

In this paper, one of a series describing the Canada-France Redshift Survey (CFRS), the question of whether the shape of the continuum in the neighborhood of an emission line can be used to identify the emission line is examined. This is of particular importance in view of the significant fraction of objects in this and other faint galaxy redshift surveys for which only a isolated emission line is seen. For emission lines at $\lambda > 6560$ Å there is a potential ambiguity between [O II] λ3727 at $z > 0.76$ and Hα at low redshift.

Many objects in the CFRS were observed on more than one occasion either by design or by accident. Each of these multiple observations was initially reduced and identified without reference to any earlier spectra, after which they were co-added (if this was advantageous). The statistics of these multiple observations are examined to determine the reliability of the spectroscopic identifications in the different confidence classes described by Le Fèvre et al. (1995, hereafter CFRS II). These repeat observations can also be used to infer the nature of some of the sources that remain unidentified in the final spectroscopic sample and to provide an estimate of the internal accuracies of the redshift measurements.

Finally, spectroscopic data are presented for a sample of 437 faint stars and galaxies with $17.5 \leq I_{AB} \leq 22.5$ in the 1415+52 and 2215+00 survey fields of the CFRS.

2. GALAXIES WITH SINGLE ISOLATED EMISSION LINES

A familiar problem for those who work in this field is how to treat objects in which the only sharp feature is a single isolated emission line superposed on a continuum. In the absence of any other identifiable absorption or emission lines, can such an emission line be reliably identified?

The CFRS sample of 1010 spectra contains 71 objects in which only a single emission line was seen. Figure 1 (*top*) shows the distribution of wavelengths of the emission line in these objects. In the majority of objects the emission line was seen toward the red end of the spectrum. While most people would accept the hypothesis that these single isolated emission lines are produced by [O II] λ3727, other possibilities exist, and in order to treat these objects as rigorously as possible, all such spectra were put to one side for the systematic analysis described below.

Figure 1 (*bottom*) shows the wavelengths of the strongest emission lines usually seen in galaxy spectra as a function of redshift within the spectral range of the CFRS spectra. A single isolated emission line at $\lambda > 4800$ Å is unlikely to be produced by one of Hβ λ4861 or [O III] $\lambda\lambda$4959, 5007. In most spectra, the Hβ line and the [O III] $\lambda\lambda$4959, 5007 doublet are usually seen as a triplet of lines (the line ratios of the latter two are fixed by atomic physics at 1:3). Furthermore, given the wide wavelength range of our spectra, either Hα or [O II] λ3727 should be visible with Hβ for all redshifts (see Fig. 1 [*bottom*]).

Turning to [O II] λ3727, this line can be seen on our spectra over a wide range of redshifts and could be expected to be the only strong feature present at $z > 0.7$ when the Hβ λ4861 and [O III] $\lambda\lambda$4959, 5007 combination moves out of the spectral range. It is noticeable and suggestive in Figure 1 (*top*) that most of the "single emission lines" are indeed seen at $\lambda > 6300$ Å corresponding, for an [O II] λ3727 identification, to just this range $z > 0.7$. The Balmer absorption lines that might be expected to be seen near [O II] λ3727 are variable in strength and can be filled in by emission. However, for lines at $\lambda > 6563$

[1] Visiting Astronomer, Canada-France-Hawaii Telescope, which is operated by the National Research Council of Canada, the Centre Nationale de la Recherche Scientifique of France, and the University of Hawaii.

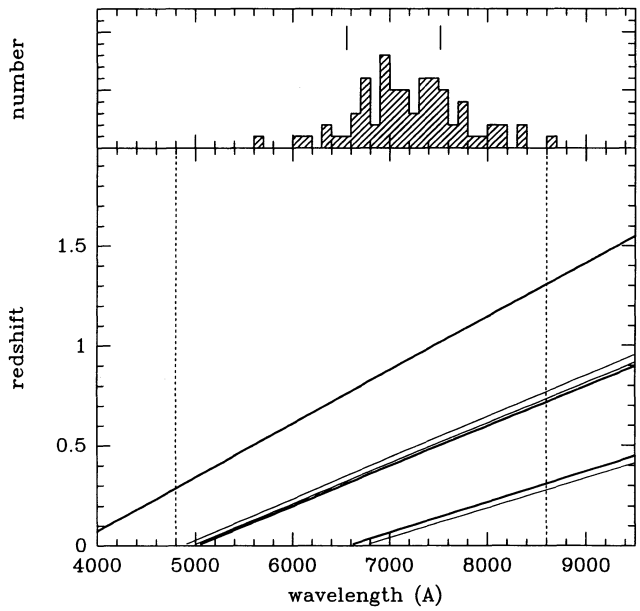

FIG. 1.—*Upper panel:* The distribution of wavelengths of the emission lines in spectra in which the only sharp feature was a single isolated emission line. The vertical bars indicate the range of wavelengths over which the analysis of the continuum shape described in the text could be performed. *Lower panel:* The wavelengths of the most prominent emission lines in the optical spectra of galaxies as a function of redshift. Vertical dashed lines show the spectral range of our spectra. These curves show (1) that [O II] λ3727 is likely to be the only emission feature visible for $0.7 < z < 1.3$ and (2) that Hα λ6563 could be confused with [O II] λ3727 for $\lambda > 6563$ Å if [S II] λ6724 and the Hβ, [O III] $\lambda\lambda$4959, 5007 lines are absent. The continuum analysis was designed to distinguish between these two possibilities.

Å, a serious potential ambiguity exists between Hα at low redshift and [O III] λ3727 at $z > 0.76$. If the line is Hα, then we might hope to see [S II] λ6724 to the red and the Hβ λ4861 and [O III] $\lambda\lambda$4959, 5007 at shorter wavelengths (see Fig. 1 [*bottom*]), but the absence of the latter cannot be taken as definitive because of the possibility of extinction. A final, more exotic, possibility is that such a line is Lyα at $z > 2$. However, for most of the single emission lines, where the line is longward of 6300 Å (see Fig. 1 [*top*]), this would make the redshift very high, $z > 4$, and would place the Lyman limit well within our spectral range, at $\lambda > 5000$ Å. At these redshifts, extrinsic as well as intrinsic H I absorption would be likely to extinguish the continuum below the Lyman limit, and the fact that this is not seen makes this identification unlikely. In addition, if the lines were Lyα, it might be expected that more such lines would be seen at $\lambda < 6300$ Å.

In the light of the above discussion, any isolated emission lines at $\lambda < 6560$ Å (a minority of the sample—see Fig. 1 [*top*]) were regarded as securely identified with [O II] λ3727. In order to secure identifications of the single emission lines at $\lambda > 6560$ Å, where there is the potential ambiguity with Hα, we have investigated whether the shape of the continuum in the neighborhood of the line could be used as a diagnostic. This was motivated by the fact that the continua of many of the single emission-line objects show a distinctive rise just redward of the line that resembles that seen in objects in which the [O II] λ3727 identification is secure on the basis of absorption lines or other emission lines. It is important to note that the wavelength and shape of this continuum feature varies since it is caused by a combination of the general Balmer break in hot stars and the well-known 4000 Å break in cooler stellar populations.

Accordingly, we defined a continuum color and break index as follows. If a single isolated emission line was observed at wavelength λ_{em}, then a straight line was fitted to the continuum (in linear units of of f_ν vs. λ) between $0.858\lambda_{em}$ and $0.966\lambda_{em}$ and between $1.073\lambda_{em}$ and $1.127\lambda_{em}$. If the line is indeed [O II] λ3727, then these ranges correspond to 3200–3600 Å and 4000–4200 Å. The upper continuum measurement is therefore above both the Balmer break and the 4000 Å break. This procedure is illustrated in Figure 2. We then calculated the flux densities at points A and B (the midpoints of these two ranges) and at point C (the extrapolation of the short wavelength continuum to $1.100\lambda_{em}$, equivalent to 4100 Å), and defined the color and break index to be

$$\text{color} = -2.5 \log_{10}\left(\frac{f_A}{f_B}\right)$$

$$\text{break} = -2.5 \log_{10}\left(\frac{f_B}{f_C}\right).$$

It should be noted that the "break index" measures the curvature of the continuum and not simply a color across a break (cf., for example, the 4000 Å break index of Hamilton 1985) and is sensitive to the presence of both the 4000 Å break and the Balmer limit at 3648 Å. With our spectra, these parameters could be measured for galaxies in which $5600 < \lambda_{em} < 7520$ Å (corresponding to $0.5 < z < 1.0$ for an [O II] λ3727 identification). Outside of this range, there was inadequate continuum longward or shortward of the line to measure these continuum parameters reliably. We measured these parameters for all the single emission lines in this range and also for all objects in which either [O II] λ3727 or Hα had been identified to lie in this same wavelength range. These latter form a

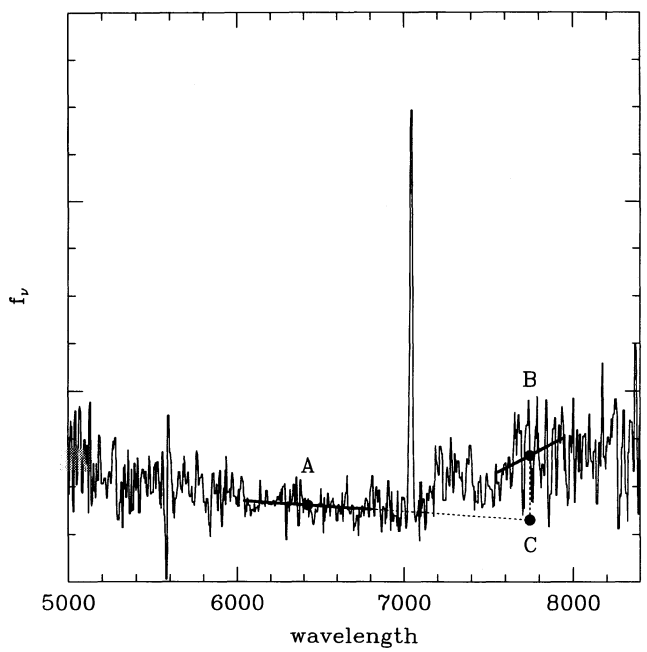

FIG. 2.—Example of a spectrum showing only a single strong emission line, indicating the continuum measurements made to derive the color and break parameters. See text for details.

"defining sample" for our algorithm. We have not attempted to determine error bars for individual measurements because of the fact that the measurements are likely to be affected by non-Poissonian effects. Rather, we take an empirical approach, using the "defining samples" to determine the range of parameters observed in the sample after the inclusion of all observational errors.

2.1. *Emission-Line Objects that Have Secure Redshifts*

Figures 3*a* and 3*b* show these parameters for two defining samples. First, in Figure 3*a* we plot those galaxies with $0.75 < z < 1.0$ that have secure [O II] λ3727 line identifications (based on other features) in the $6560 < \lambda_{em} < 7520$ Å range. The measurements in this sample thus span exactly the same wavelength range as in the target sample and thus will reflect to precisely the same degree any problems encountered in defining the continua in the spectra. However, this defining sample may, by definition, be missing prototypes of the objects in which only a single line can be seen. Therefore, in Figure 3*b*, we plot all emission-line galaxies (including the single emission-line objects) lying between $0.5 < z < 0.75$, i.e., with $5600 < \lambda_{em} < 6560$ Å (where the line cannot be Hα). *These galaxies must span the full range of the population.* The greater scatter in this sample is probably due to the difficulties of measuring the continuum slope at short wavelengths in our spectra. Finally, we plot on both diagrams low-redshift galaxies in which Hα was observed at $\lambda < 7520$ Å.

On both diagrams there is a clear separation between the high-redshift [O II] λ3727 emitters and the low-redshift Hα emitters—the latter do not show a break feature and are also

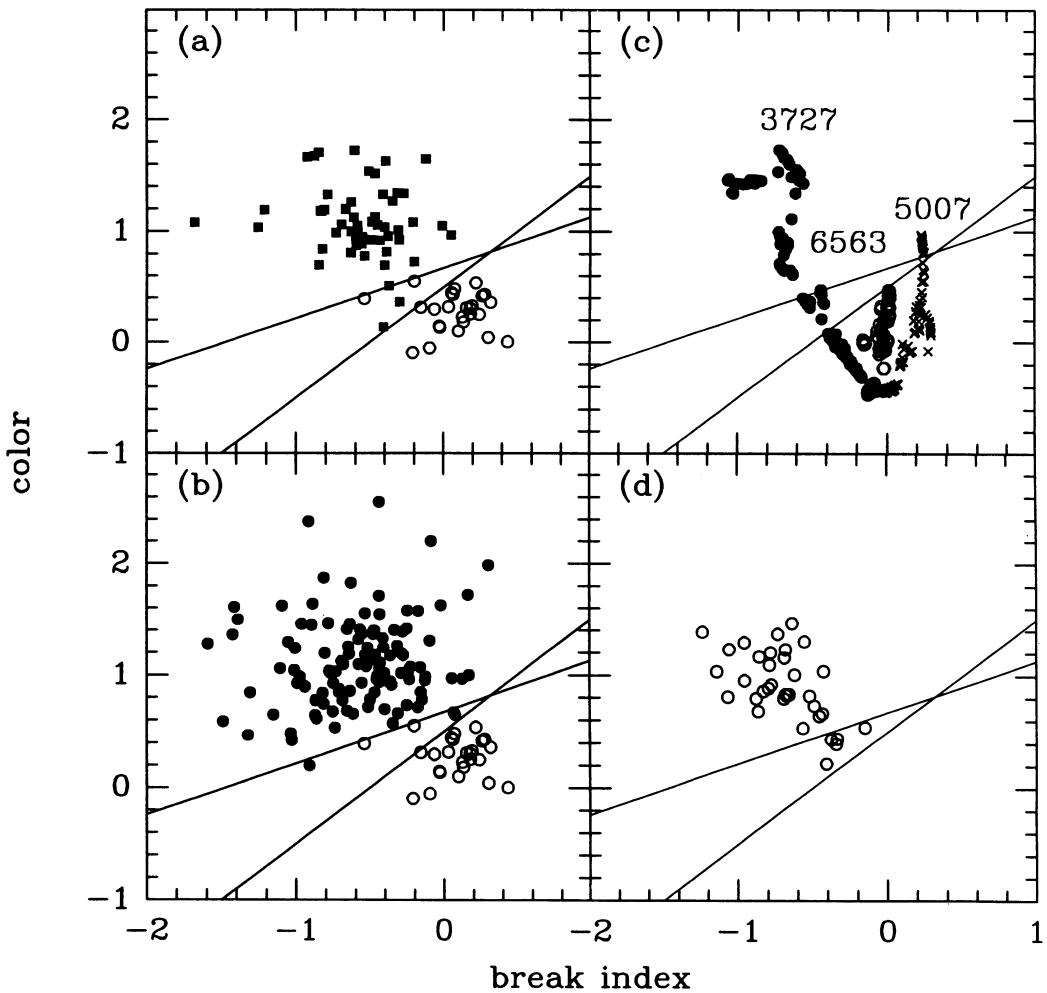

FIG. 3.—The break and color indices of the continuum around an emission line, as defined in the text, are plotted for three samples of galaxies and for a set of synthetic galaxy spectra from the GISSEL library. Panel (*a*) shows galaxies with secure $0.76 < z < 1.03$ in which the emission line is securely identified with [O II] λ3727 on the basis of other spectral features (*filled squares*) and galaxies with secure $0.0 < z < 0.15$ in which the line is securely identified with Hα (*open circles*). Panel (*b*) is the same as (*a*) except that the high-redshift sample now consists of all galaxies with $5590 < \lambda_{em} < 6560$, i.e. $0.5 < z < 0.76$, in which the emission line cannot be Hα. The increased scatter is due to the difficulty of measuring the continuum at the shorter wavelengths. These two panels both indicate a separation between these indices for spectra in which the line is [O II] λ3727 and those in which the line is Hα with only a small region of ambiguity (between the sloping lines). Panel (*c*) shows the indices for a wide range of synthetic spectra generated by the GISSEL package assuming that an emission line is [O II] λ3727 (*open circles*), [O III] λ5007 (*crosses*), and Hα (*small dots*), respectively. Except for some degeneracy for very blue spectra (i.e., the youngest model galaxies), the three possibilities occupy separate loci on the diagram. Panel (*d*) shows the parameters of the test sample consisting of galaxies with only a single emission line. The vast majority of these are in the area occupied by the [O II] λ3727 identifications with only a few in the ambiguous area. The scatter in this plot would be expected to be comparable to that in panel (*a*). See text for further details and discussion.

generally bluer in this color. The lines shown on Figure 3 define regions where, empirically, the lines are exclusively identified with [O II] λ3727 and Hα, respectively, plus an intermediate, ambiguous, region.

2.2. *Model Spectra*

Theoretical models support this empirical analysis. In Figure 3*c* we plot the same indices calculated for a wide range of spectral energy distributions of model galaxies produced by the GISSEL spectral synthesis code of Bruzual & Charlot (1993) with λ_{em} set to 3727 Å, 5007 Å, and 6563 Å, respectively (we are greatly indebted to Gabriela Mallen-Ornelas for performing these model computations). In Figure 3*c* we show the color and break indices for the models for the three different λ_{em} values. As expected, although there is degeneracy for the bluest models (very young galaxies have blue featureless spectra over a wide wavelength range), the continua around 3727 Å rapidly develop a significant break and separate from the 5007 Å and 6563 Å models in the figure, supporting the empirical evidence from Figures 3*a* and 3*b*.

2.3. *Application to Single Emission-Line Objects*

Finally, in Figure 3*d*, we plot the indices for the 35 single emission-line objects with $6560 < \lambda_{em} < 7520$ Å, i.e., the target sample for which we hope to use the continuum shape to secure the line identification. Apart from five galaxies that lie in the overlap region, these objects lie in the area in which the emission line is identified with [O II] λ3727. Based on this, the 30 galaxies in the [O II] area were assigned to a confidence class of 8 (see CFRS II), and we treat them as securely identified at the redshift obtained by identifying the line as [O II] λ3727. The other five were assigned a confidence class of 9 and provisionally also placed at the higher redshifts, although the lower Hα-based redshift cannot be ruled out.

We were unable to use the continuum shape in this way for (1) single emission-line objects in which the emission line lay at $\lambda_{em} > 7520$ Å, where we have inadequate long wavelength continuum to reliably determine the break and color indices and (2) the handful of MARLIN spectra with $6563 < \lambda_{em} < 7520$ where the continua were less reliable due to poorer flux calibration. We have assigned these 24 objects also to class "9".

However, the fact that in those objects for which we *could apply* this continuum-based criterion, the line was to a very large degree identified with [O II] λ3727 (85% secure identifications and the remainder ambiguous), which suggests that *most* of the emission lines in the remaining 29 class 9 objects, where we could not apply this test or where the test was ambiguous, are also likely to be associated with [O II] λ3727, and we will generally make this assumption in future papers.

The high degree of association between single isolated emission lines and [O II] λ3727 is consistent with the idea that Hα should be accompanied by other emission lines (e.g., Hβ and [O III] $\lambda\lambda$4959, 5007) or absorption lines (e.g., Mg *b* λ5175) leading to a secure identification.

3. ANALYSIS OF REPEAT OBSERVATIONS

During the course of this project, 187 objects were observed spectroscopically on more than one occasion. These repeat observations were made (1) because the first spectrum had not resulted in an identification, (2) in order to verify identifications of low confidence class, or (3) in a few cases, by mistake. Regardless of the motivation, the new spectra were reduced and identified in the manner described in CFRS II without knowledge of what the earlier identification had been or even, in most cases, whether the observation was even a repeat. After the analysis of the new spectrum was finalized, the two (or more) spectra of each object were then compared, co-added if this was deemed advantageous, and a final identification and confidence class assigned. In some cases the co-added spectra reinforced the original identifications, and in these cases the confidence class was sometimes increased. In a few cases, the co-added spectra did not support the original identifications, particularly if the original identifications were discrepant, and in this case the confidence class could be decreased and/or the object regarded as unidentified.

The fact that each observation was initially treated quite independently of any earlier ones means that these repeat observations allow a number of empirical tests of the data to be made, and these are described below.

3.1. *Empirical Calibration of the Reliability of the Confidence Classes*

Of the 187 objects observed more than once, 91 were independently identified (with a confidence class of 1, 2, 3, 4, 8, or 9 or the quasar classes 12, 13, or 14—see CFRS II) more than once. These objects thus provide an empirical calibration of the reliability of identifications in these confidence classes.

This analysis was carried out as follows: For each individual independent identification in turn, we asked whether this identification was either confirmed or refuted by another identification with equal or higher confidence class, defining this to be a "test." We thus disregarded all identifications made at lower confidence as not significantly testing the higher confidence identification. Where both observations had the same confidence class we regarded this as two "tests." In the case in which the two identifications agreed, we counted this as two "successes." If they disagreed, then we compared each with the final identification obtained from co-adding both spectra (regardless of its confidence class). This sometimes led to one "success" and one "failure" but sometimes to two "failures" if the co-added spectra supported neither identification and the object had been finally classified as unidentified. As a final complication, the "single emission line" classes 8 and 9 (see § 2) were regarded as both confirming, and being confirmed by, confidence classes 2, 3, and 4. Under these criteria, we had 147 separate "tests."

The results of these tests are shown in Table 1. The verification rates for the main classes increase monotonically from 56% for class 1 (not regarded as a secure identification) up to 100% for class 4. The verification rates for classes 2 and 3 (81% and 97%, respectively) may in fact be underestimates, since

TABLE 1

EMPIRICAL VALIDATION OF CONFIDENCE CLASSES

Confidence Class	Percent of Complete Sample	Number of "Tests"	Number of Successes	Success Rate
4	35	23	23	100%
8 and 9.....	6	20	20	100
3	33	38	37[a]	97
2	10	32	26[b]	81
1	6	34	19	56

[a] Single failure was a quasar originally misidentified as a lower redshift galaxy.

[b] Four of these six failures are due to two objects that failed twice (see text).

four of the six failures in the class 2 category come from just two objects (in which neither of the two original class 2 identifications were supported by the co-added spectra), and the single failure in class 3 is a rather pathological object. It is one of the few quasars in the sample and the Mg λ2799 line at $z = 1.35$ was initially mistakenly identified in an earlier spectrum as [O III] λ5007 at lower redshift. Finally it should be noted that the emission lines in the single emission-line objects were *invariably* confirmed in repeated observations, indicating that our discrimination against cosmic rays was successful. In some cases, the redshift was secured by the identification of other supporting features.

As described in CFRS II, the confidence class scheme was set up at the start of the project to describe, as well as possible, the likelihood that each claimed identification was correct. Reassuringly, the empirical verification rates found in this analysis reflect our original a priori definition of these probabilities.

3.2. *Redshift Accuracy*

A total of 48 galaxies were identified at confidence class 2 or higher from more than one observation. The differences in the measured redshifts from these independent spectra therefore give an empirical estimate of the accuracy of the redshifts in the survey. The histogram of redshift differences is shown in Figure 4. There is a broad peak out to $\Delta z = 0.002$ with only a few outliers beyond. The r.m.s. redshift difference is nominally 0.0026 implying a redshift r.m.s. uncertainty per observation of 0.0019 or a velocity uncertainty of 570 km s^{-1}. The true uncertainty is likely to be smaller. Elimination of the outliers with $\Delta z > 0.005$ yields an r.m.s. difference of 0.00185, or an r.m.s. uncertainty of 0.0013. An uncertainty of 0.0013 is also obtained by considering the differences in the redshifts of only the highest quality spectra (confidence class 4). This is equivalent to a velocity uncertainty of 390 km s^{-1}.

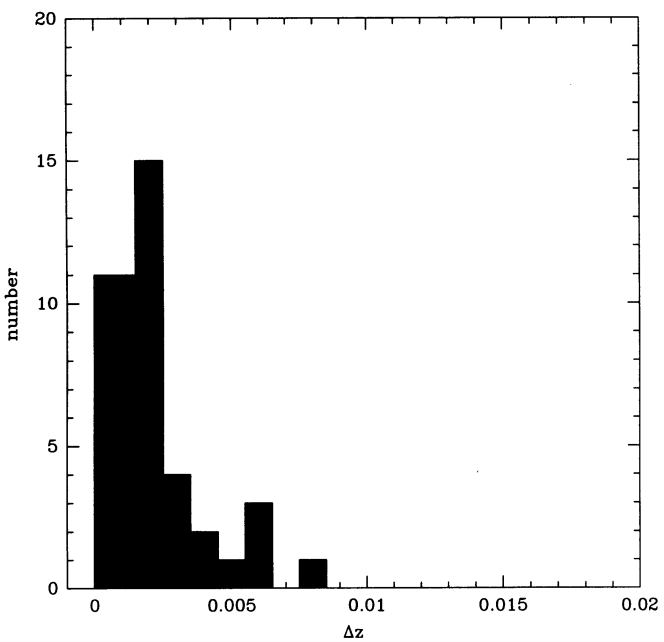

FIG. 4.—Histogram of redshift differences $|\Delta z|$ derived from multiple observations of galaxies.

3.3. *Recovery of Initial Failures*

A final statistic of interest is how often a repeat observation of an initial "failure" (i.e., an object for which no identification could be made from a single 8 hr spectrum) led to its eventual secure identification, either from the new spectrum alone or through the co-addition of the two spectra. Accordingly, we examined the *final* identification status of the 99 objects with repeated observations in which one observation had failed to identify the object securely (i.e., with confidence class 0 or 1). In 70 of these 99 objects (70%) the additional data resulted in a secure identification in the final catalog (i.e., with confidence class 2 or greater).

The significance of this statistic is that it means that many of the objects in the final catalog that were not identified and that were not reobserved could presumably have been successfully identified with repeat observations. Furthermore, if it is assumed that the failures that were reobserved are representative of the failures that were not reobserved, then we can use the identifications of the objects "recovered" by the repeat observations to estimate, at least in a statistical sense, the nature of 70% of the failures that were not reobserved. This aspect is developed in Crampton et al. (1995, hereafter CFRS V).

4. SPECTROSCOPIC DATA IN THE 1415+52 AND 2215+00 SURVEY FIELDS

Tables 2 and 3 present spectroscopic identifications for objects in the 1415+52 and 2215+00 survey fields. The columns in Tables 2 and 3 are (1) identification number; (2) right ascension [2000.0]; (3) declination [2000.0]; (4) isophotal I_{AB} magnitude; (5) $(V-I)_{AB}$ color; (6) the Q compactness parameter (see Lilly et al. 1995, hereafter CFRS I); (7) the redshift, with 9.999 indicating an unidentified object and 0.000 indicating a star; (8) the confidence class (see CFRS II); and (9) the spectroscopic features identified. A "1" indicates the general continuum shape supported the identification. A "2" represents the features of an M star. Figures 5 and 6 (Plates 5–6) show gray-scale representations of the I-band images of these fields, and Figures 7 and 8 identify those objects listed in Tables 2 and 3.

In the 1415+52 field there are 224 objects in the statistically complete sample plus an additional 14 objects in the supplementary catalog (see CFRS II for a definition of the latter). The photometric catalog in the 1415+52 field contains 560 objects with $17.5 < I_{AB} < 22.5$, so the sampling rate is approximately 40%. The 1415+52 field benefited from a prolonged sequence of observations allowing reobservations of unidentified objects. Of the 224 objects in the statistically complete sample, only 27 remain unidentified (i.e., classes 0 and 1), and the spectroscopic identification rate in this field is thus 88% (the highest in the CFRS survey). The fraction of stars is 21%. We have been able to identify many of the faint galaxies in this field with faint microjansky radio sources from Fomalont et al. (1991), and these are discussed in Hammer et al. (1995b, hereafter CFRS VII). Le Fèvre et al. (1994) have described a structure of over a dozen galaxies at $z = 0.985$ in this field. The overall redshift distribution in this field is shown in Figure 9.

As discussed in CFRS V, examination of the colors and morphologies of two objects in the 1415+52 field, 14.0664 and 14.0823, indicate that they were misclassified spectroscopically as early-type galaxies at $z \sim 0.3$ when in fact they are almost certainly K stars. Interestingly, the spectra of these two objects, and only these two, had been flagged as suspicious during a

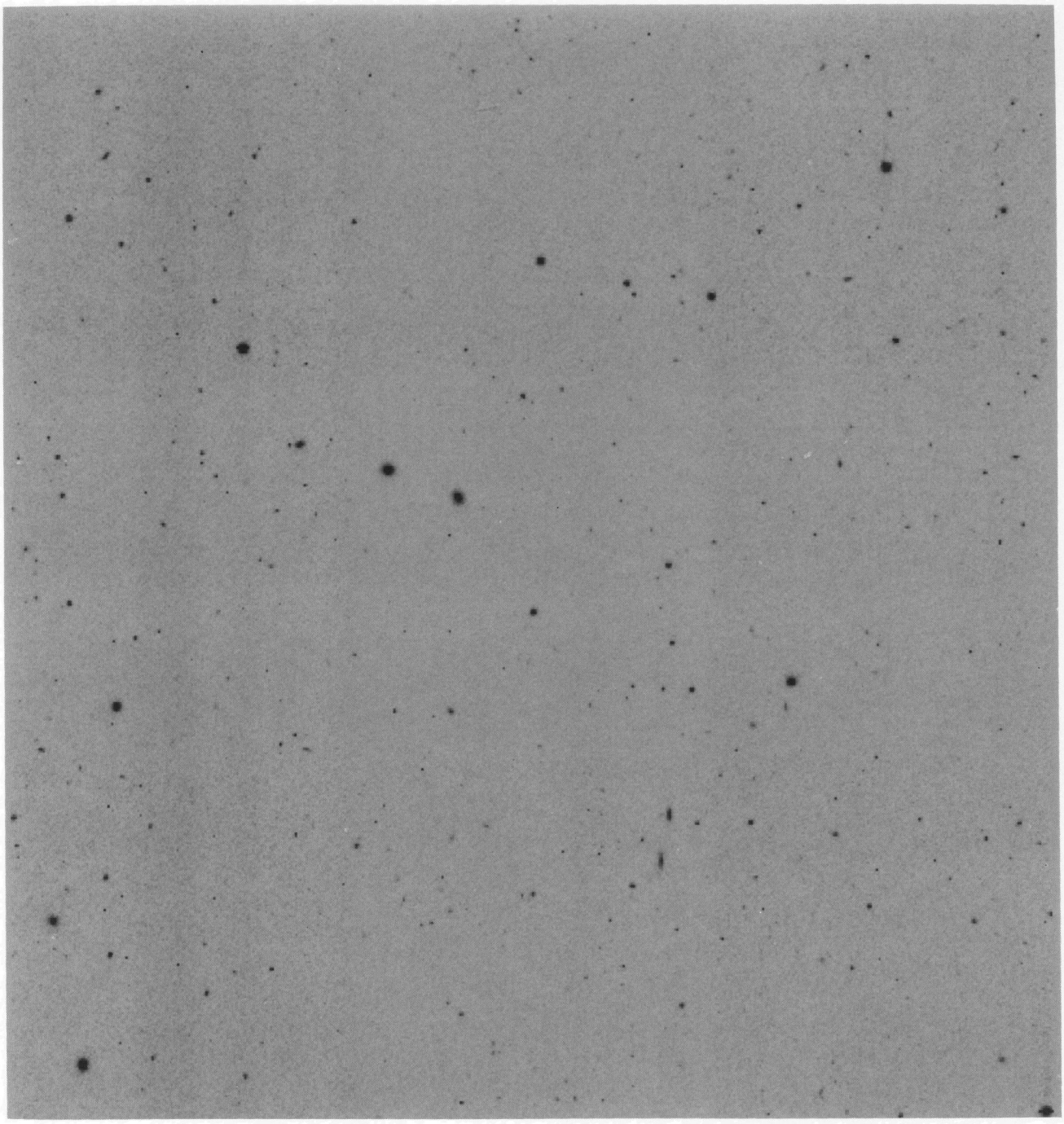

FIG. 5.—Gray-scale representation of the 1415 + 52 field. North is at top, and east is to the left. Field is 10 × 10 arcmin^2.

LILLY et al. (see 455, 79)

PLATE 6

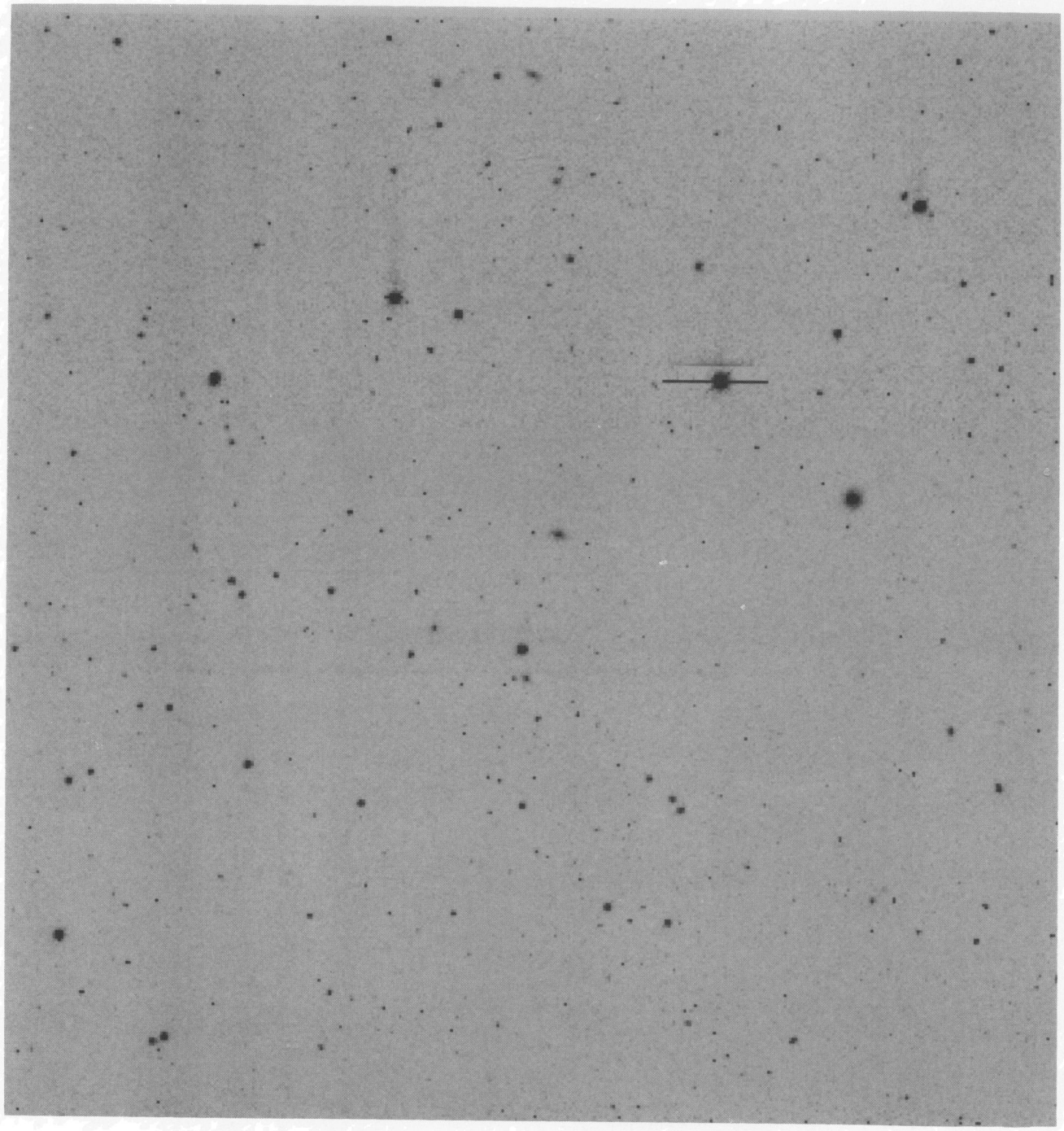

FIG. 6.—Gray-scale representation of the 2215+00 field. North is at top, and east is to the left. Field is 10 × 10 arcmin².

TABLE 2

SPECTROSCOPIC CATALOG IN THE 1415+52 FIELD

CFRS	RA[2000]	δ[2000]	I_{AB}[a]	$(V-I)_{AB}$[b]	Q[c]	z	C[d]	Spectroscopic features [e]
14.0020	14 18 23.71	+52 30 09.7	21.09	1.76	0.87	0.0000	4	2
14.0024	14 18 23.64	+52 29 56.9	20.67	1.11	4.36	0.5313	4	3727 3933 3969 4102 1
14.0025	14 18 23.61	+52 30 16.7	21.16	0.32	2.65	0.2358	4	4000 4863 4959 5007 6562 6725
14.0027	14 18 23.53	+52 26 33.0	21.80	0.58	1.68	0.2000	2	5175
14.0028	14 18 23.49	+52 27 33.1	21.70	0.75	1.86	···	0	
14.0068	14 18 22.02	+52 26 02.5	22.13	0.38	1.83	0.2130	1	
14.0070	14 18 21.92	+52 27 24.0	20.73	0.24	5.07	0.0642	4	4863 4959 5007 6562 6725
14.0071	14 18 21.83	+52 30 31.6	22.00	1.79	0.86	0.0000	4	2
14.0072	14 18 21.79	+52 31 06.8	22.46	0.91	0.91	0.6172	4	3727 3868 3969 4340 4863 4959 5007
14.0077	14 18 21.61	+52 29 54.0	17.94	2.74	0.98	0.0000	4	2
14.0117	14 18 19.62	+52 34 23.7	18.66	0.96	2.79	0.2020	2	3933 3969 4000 5175 5892
14.0119	14 18 19.62	+52 29 00.0	22.41	1.42	2.25	···	0	
14.0122	14 18 19.53	+52 27 30.4	19.25	1.05	2.34	0.2820	4	3933 3969 4304 4863 5175 5892
14.0129	14 18 19.18	+52 30 41.0	22.41	1.01	1.94	0.9023	3	3727 3969 4102 4340 1
14.0130	14 18 19.05	+52 34 06.5	21.53	1.17	2.28	0.5641	2	3727 3969 4102 4304
14.0143	14 18 18.47	+52 34 14.9	20.12	2.06	0.92	0.0000	4	2
14.0144	14 18 18.51	+52 30 40.5	22.97	0.72	1.08	0.9000	93	3727 3969
14.0145	14 18 18.57	+52 27 20.0	21.59	1.48	0.82	0.0000	3	2
14.0147	14 18 18.49	+52 30 04.0	22.41	0.20	3.63	1.1810	9	
14.0154	14 18 18.14	+52 26 33.0	22.08	0.58	1.71	1.1583	9	3727
14.0159	14 18 17.61	+52 32 50.4	22.46	2.09	1.09	···	0	
14.0163	14 18 17.59	+52 29 36.3	18.94	2.00	0.91	0.0000	4	2
14.0166	14 18 17.28	+52 33 38.8	22.31	2.64	2.10	0.6880	92	3969 4304
14.0180	14 18 16.87	+52 30 52.7	21.76	0.94	1.20	0.5684	3	3727 3969 4102 4863 5007
14.0185	14 18 16.76	+52 27 57.2	19.94	1.29	3.96	0.3730	3	4000 4304 5175
14.0187	14 18 16.60	+52 33 37.4	18.17	1.20	1.09	0.0000	94	5175
14.0189	14 18 16.69	+52 25 55.4	20.24	1.10	2.84	0.0000	1	2
14.0198	14 18 16.16	+52 29 39.7	20.04	0.17	1.02	1.6034	14	1909 2799
14.0207	14 18 15.84	+52 30 35.6	19.42	1.92	2.38	0.5460	4	3933 3969 4000 4102 4304 4863 5175
14.0208	14 18 15.79	+52 32 55.7	21.74	0.39	2.95	0.2003	4	4959 5007 6562 6725
14.0217	14 18 15.38	+52 33 59.3	21.73	1.00	1.58	0.7168	3	3727 3969
14.0227	14 18 15.16	+52 31 19.3	20.84	1.24	4.32	0.7720	3	3885 3969 4102
14.0233	14 18 15.14	+52 26 44.4	21.68	1.86	0.87	0.0000	4	2
14.0256	14 18 14.14	+52 34 26.2	21.00	1.80	0.90	0.0000	4	2
14.0265	14 18 13.78	+52 33 12.2	20.68	0.71	1.79	0.3224	4	3727 3969 4102 4340 4863 5007 5175
14.0272	14 18 13.48	+52 31 46.2	20.51	1.19	3.63	0.6678	3	3727 3969 4000 4102
14.0279	14 18 13.39	+52 26 29.5	19.19	1.11	2.87	0.2760	4	4304 5175 6214
14.0297	14 18 12.58	+52 31 01.4	19.47	0.09	0.95	0.0000	4	4863 6562
14.0308	14 18 11.90	+52 30 52.9	21.27	2.03	0.89	0.0000	4	2
14.0310	14 18 11.93	+52 29 14.7	20.96	0.34	3.50	0.2384	4	3727 3969 4304 4863 4959 5007 6562 6725
14.0315	14 18 11.65	+52 26 40.2	20.64	0.73	3.99	0.4276	93	3727 3969 4304 5007
14.0321	14 18 11.19	+52 33 27.3	22.06	0.57	2.28	0.2207	4	4102 4959 5007 6562 6725
14.0327	14 18 11.08	+52 26 17.3	21.95	0.83	3.32	···	0	
14.0344	14 18 10.77	+52 30 57.2	21.27	1.96	2.31	0.7210	1	3933 3969 4102 4304
14.0367	14 18 10.09	+52 33 50.0	18.38	0.34	0.93	0.0000	3	4863 5892 6562
14.0373	14 18 10.06	+52 26 47.2	21.74	1.07	1.91	0.8347	3	3837 3727 3969 4102
14.0377	14 18 09.91	+52 30 16.9	20.95	0.36	1.89	0.2596	4	3727 4863 4959 5007 6562
14.0384	14 18 09.49	+52 29 18.9	22.10	0.77	0.89	0.0000	2	5175 6562
14.0389	14 18 09.32	+52 33 14.5	23.33	0.89	1.13	0.8906	98	3727
14.0391	14 18 09.41	+52 26 41.8	19.07	0.63	1.05	0.0000	3	5175
14.0393	14 18 09.22	+52 30 13.4	20.44	0.98	3.91	0.6016	4	3727 3969 4102 4863 5007
14.0403	14 18 08.87	+52 30 42.8	20.61	1.77	3.10	0.7139	3	3727 3933 3969 4000 4304
14.0422	14 18 08.03	+52 31 17.4	20.34	1.45	1.94	0.4210	2	3969 4102 4304 4863
14.0429	14 18 07.59	+52 34 27.6	22.14	2.01	1.49	0.6450	2	3933 3969 4102 4304
14.0435	14 18 07.41	+52 31 17.9	17.97	0.71	6.73	0.0684	3	4340 4863 5175 5892 6562
14.0438	14 18 07.32	+52 26 48.8	21.39	0.74	2.61	0.9862	8	3727 3969
14.0440	14 18 07.22	+52 30 29.0	21.80	1.89	1.90	0.9896	2	3933 3969 4000 4102
14.0443	14 18 07.09	+52 30 56.4	20.19	2.08	0.83	0.0000	4	2
14.0449	14 18 07.05	+52 27 23.9	22.22	2.38	1.84	···	0	
14.0456	14 18 06.74	+52 26 19.4	22.05	0.67	1.29	0.5787	3	3727 4863 5007
14.0462	14 18 06.43	+52 32 57.9	22.31	2.54	0.88	0.0000	3	2
14.0473	14 18 06.16	+52 34 23.5	21.25	2.16	3.12	0.6463	3	3727 4000 1
14.0485	14 18 05.81	+52 29 22.4	22.16	0.83	2.23	0.6545	3	3727 3969 4102 4340
14.0487	14 18 05.77	+52 30 47.7	22.36	0.90	2.03	0.8026	8	3727
14.0497	14 18 05.30	+52 30 27.3	21.69	1.10	2.27	0.7970	3	3727 1
14.0516	14 18 04.64	+52 30 59.2	22.44	2.29	0.95	···	0	
14.0528	14 18 04.19	+52 29 26.9	20.61	0.20	2.02	0.0640	4	4863 4959 5007 6562 6725
14.0529	14 18 04.04	+52 33 15.3	18.23	1.97	0.86	0.0000	4	2
14.0538	14 18 03.96	+52 25 51.8	21.82	0.57	1.96	0.8085	8	3727 3869
14.0542	14 18 03.58	+52 34 23.0	21.51	1.69	2.64	0.7200	3	4000 4102 4304
14.0543	14 18 03.74	+52 26 59.2	20.56	1.43	0.99	0.0000	4	2
14.0547	14 18 03.47	+52 30 21.7	21.07	0.67	4.15	0.2270	1	3727 6562 6725
14.0555	14 18 02.94	+52 34 32.7	20.34	1.68	1.12	0.0000	4	2
14.0566	14 18 02.51	+52 25 54.0	22.04	1.82	1.35	0.9954	2	3737 break
14.0573	14 18 02.02	+52 31 04.5	16.90	0.19	7.48	0.0100	94	4863 4959 5007 6562 6725 7330
14.0574	14 18 02.04	+52 29 54.4	21.39	0.51	1.14	0.0000	2	6562 1
14.0579	14 18 01.73	+52 28 57.5	19.75	2.14	1.00	0.0000	4	2
14.0580	14 18 01.71	+52 27 29.0	20.70	1.45	4.78	0.7440	3	3933 3969 4102 4304 4340
14.0581	14 18 01.48	+52 34 21.7	21.54	1.36	3.03	0.6600	2	3933 3969 4102 4304 1
14.0588	14 18 01.32	+52 27 17.9	20.58	0.34	4.82	0.0992	4	4863 4959 5007 6300 6562 6725
14.0593	14 18 01.06	+52 31 48.4	22.12	0.64	2.14	0.6143	3	3727
14.0600	14 18 00.90	+52 32 38.4	21.53	0.69	3.39	1.0385	3	2799 3727 3885 1
14.0605	14 18 00.81	+52 26 25.0	22.44	0.40	1.73	0.8348	8	3727

TABLE 2—*Continued*

CFRS	RA[2000]	δ[2000]	I_{AB}[a]	$(V-I)_{AB}$[b]	Q[c]	z	C[d]	Spectroscopic features [e]
14.0620	14 18 00.07	+52 32 06.4	22.08	2.30	0.99	0.0000	3	2
14.0621	14 18 00.18	+52 27 04.9	21.18	0.32	2.29	0.2871	4	3727 3885 3969 4863 4959 5007 5175 6562
14.0651	14 17 58.84	+52 31 38.8	21.96	1.64	1.35	0.6370	1	3969 4000 4102 4304
14.0652	14 17 58.92	+52 27 29.7	21.27	0.09	0.92	0.0000	2	4861 5892 6563
14.0656	14 17 58.66	+52 26 23.9	21.30	1.72	2.20	0.7166	1	3727 3835 3933
14.0660	14 17 58.42	+52 33 31.7	22.16	1.29	3.12	0.9812	2	3727 1
14.0663	14 17 58.45	+52 27 12.4	20.88	1.46	2.72	0.7434	4	3727 3885 3969 3933 4102 4304 4340 4863
14.0664	14 17 58.37	+52 29 39.0	21.38	0.76	0.78	0.0000	2	5175
14.0666	14 17 58.29	+52 30 29.8	21.29	1.82	1.01	0.0000	4	2
14.0685	14 17 57.72	+52 30 49.9	17.19	0.74	4.43	0.0810	94	3933 3969 4863 5175 5892 6562
14.0692	14 17 57.45	+52 33 39.8	22.18	0.75	1.61	0.4830	3	3727 3969 4102 4340 4863a
14.0697	14 17 57.44	+52 27 13.7	22.14	0.61	0.90	0.8271	93	3727 3869 3969 4304
14.0725	14 17 56.19	+52 30 44.0	22.32	1.48	1.68	0.5820	3	3727 4863 5007
14.0727	14 17 56.22	+52 27 57.0	20.61	0.85	3.66	0.4638	3	3727 3969 4102 5007
14.0739	14 17 55.89	+52 26 02.7	20.59	1.64	4.01	0.6806	3	3933 3969 4102
14.0746	14 17 55.50	+52 31 52.8	21.62	2.00	1.34	0.6750	3	3885 3933 3969 4000 4102 4304 4863
14.0753	14 17 55.32	+52 27 24.3	22.28	0.55	2.12	0.5472	4	3727 3868 4102 4340 4959 5007
14.0757	14 17 55.00	+52 33 40.6	22.29	0.77	2.34	0.9921	8	3727
14.0760	14 17 55.04	+52 29 19.7	22.09	0.39	0.88	···	0	
14.0779	14 17 54.29	+52 33 57.6	22.01	1.09	1.64	0.5781	4	3727 3969 4102 4863
14.0792	14 17 53.76	+52 34 23.3	20.76	1.90	1.90	0.6797	3	3933 3969 4102 4304
14.0807	14 17 53.56	+52 29 22.8	21.88	1.22	1.75	···	0	
14.0818	14 17 53.37	+52 25 49.4	21.02	1.12	3.46	0.8990	3	3727 3835 3885 3969 4102
14.0821	14 17 53.16	+52 29 49.3	17.06	1.01	1.08	0.0000	94	5175 5892 6880
14.0823	14 17 53.20	+52 27 02.8	21.43	0.92	0.87	0.0000	2	5175
14.0824	14 17 52.99	+52 33 03.2	22.48	1.24	2.22	0.5155	2	3727 1
14.0846	14 17 52.11	+52 30 52.7	21.81	1.34	3.68	0.9889	92	3426 3868 3727
14.0848	14 17 51.97	+52 31 20.3	22.30	0.99	1.83	0.6622	3	3727 3969 4959 5007
14.0851	14 17 51.98	+52 28 35.8	22.15	1.49	1.17	···	0	
14.0854	14 17 51.90	+52 29 29.5	21.50	2.23	2.32	0.9920	2	3885 3933 3969 4102
14.0875	14 17 51.42	+52 25 42.6	22.49	1.01	1.19	···	0	
14.0899	14 17 50.53	+52 27 45.6	21.66	0.11	3.37	0.8750	9	3727
14.0909	14 17 50.01	+52 33 42.5	22.34	1.96	1.91	0.9779	3	3727 3885 3969 4102
14.0910	14 17 50.05	+52 32 36.9	20.77	2.88	1.11	0.0000	4	2
14.0912	14 17 50.19	+52 26 37.3	21.04	1.58	1.85	0.5461	3	3727 3933 3969 4304 5007 5157
14.0916	14 17 49.78	+52 29 00.0	21.03	0.51	2.16	0.3248	3	3727 3969 5007 5175
14.0917	14 17 49.77	+52 25 48.7	22.34	2.13	1.55	···	0	
14.0922	14 17 49.44	+52 31 56.5	22.08	3.03	1.18	0.0000	4	2
14.0962	14 17 48.14	+52 31 17.6	20.89	2.02	2.26	0.7534	2	3727 3933 3969 4304
14.0966	14 17 47.85	+52 33 38.0	21.90	0.48	3.61	0.4426	3	3727 3969 4863 5007
14.0971	14 17 47.89	+52 26 42.6	20.90	0.29	0.93	0.0000	4	5175 5892 6562
14.0972	14 17 47.76	+52 30 47.8	21.17	0.82	1.91	0.6743	4	3727 4863 4959 5007
14.0985	14 17 47.44	+52 29 24.6	22.45	1.26	1.39	0.8073	3	3727 3969 4102 1
14.0987	14 17 47.40	+52 25 56.1	21.70	1.62	1.67	0.6117	3	3727 3933 3969 4304 5175
14.0998	14 17 47.13	+52 29 10.3	20.58	1.26	2.46	0.4300	1	3727 3969
14.1002	14 17 46.86	+52 34 19.3	21.10	0.34	1.04	0.0000	2	5175
14.1003	14 17 46.82	+52 32 36.2	18.66	1.52	1.03	0.0000	4	2
14.1012	14 17 46.20	+52 30 43.7	21.41	0.82	1.81	0.4788	3	3727 3969 4102 4304 4863 5007
14.1017	14 17 46.27	+52 26 35.8	22.48	0.74	2.85	0.6020	1	3727 3969 4102
14.1028	14 17 45.88	+52 30 32.5	21.57	2.27	1.61	0.9876	3	3727 3969
14.1032	14 17 45.56	+52 34 03.3	22.39	1.62	2.14	0.6700	2	4000 1
14.1034	14 17 45.73	+52 27 12.8	21.84	0.99	2.31	0.8123	8	3727 1
14.1036	14 17 45.42	+52 34 24.0	22.36	1.56	1.81	···	0	
14.1037	14 17 45.55	+52 30 06.8	21.42	1.15	2.32	0.5489	3	3727 3969 4102 4863
14.1039	14 17 45.53	+52 27 38.1	19.29	0.31	5.74	0.0793	4	4863 4959 5007 6562 6725
14.1042	14 17 45.37	+52 29 51.2	21.49	1.89	1.49	0.7217	3	3727 5007 1
14.1043	14 17 45.27	+52 29 08.5	20.05	1.71	3.21	0.6410	4	3933 3969 4340
14.1052	14 17 44.86	+52 30 13.5	17.36	2.18	0.97	0.0000	94	2
14.1058	14 17 44.70	+52 31 06.5	23.03	0.02	1.43	0.2333	94	3727 4863 4959 5007 6562
14.1060	14 17 44.67	+52 29 32.9	18.62	0.91	0.99	0.0000	4	5175
14.1064	14 17 44.59	+52 27 02.2	20.71	0.49	2.63	0.3353	4	3969 4863 4959 5007
14.1067	14 17 44.37	+52 32 15.1	22.59	1.11	2.82	0.6598	93	3727 4102 4304 4863 5007
14.1068	14 17 44.33	+52 32 01.6	20.01	2.28	1.09	0.0000	4	2
14.1071	14 17 44.28	+52 30 19.9	22.48	0.61	1.55	0.3595	3	3727 4959 5007
14.1079	14 17 44.11	+52 28 44.7	21.95	1.37	2.29	0.9011	9	3727
14.1080	14 17 43.97	+52 32 49.0	20.34	0.34	7.55	0.0664	4	4863 5007 6562 6725
14.1081	14 17 44.17	+52 26 17.3	22.24	0.87	1.90	0.5270	1	3727 3933 3969 4102
14.1082	14 17 43.89	+52 32 32.1	20.31	0.97	3.06	0.2620	4	4000 4304 5175 6562 1
14.1087	14 17 43.73	+52 30 21.6	22.06	0.83	1.55	0.6595	3	3727 3837 3885 3969
14.1103	14 17 43.33	+52 28 05.9	22.33	0.31	0.85	0.2092	4	3967 4102 4340 5876 4863 4959 5007 6562
14.1105	14 17 43.27	+52 27 58.0	19.18	2.05	0.94	0.0000	4	2
14.1107	14 17 43.04	+52 34 23.7	22.17	1.72	1.07	0.0000	2	2
14.1116	14 17 42.65	+52 33 58.7	20.47	2.13	0.83	0.0000	4	2
14.1118	14 17 42.71	+52 30 56.0	22.48	1.00	1.10	0.9835	8	3727
14.1122	14 17 42.61	+52 31 13.5	21.97	0.99	3.82	0.6565	3	3727 3969 4102
14.1126	14 17 42.71	+52 27 29.8	22.26	0.64	2.44	0.7426	3	3727 3868 3969 4102 4304
14.1131	14 17 42.23	+52 33 23.7	22.15	0.95	2.17	0.7193	92	3727 1
14.1136	14 17 42.11	+52 29 59.4	21.61	0.76	2.65	0.6404	3	3727 3869 5007
14.1139	14 17 42.04	+52 30 25.6	20.20	1.29	3.10	0.6600	3	3727 3835 3969 4102 4340
14.1143	14 17 42.01	+52 29 24.5	22.56	0.97	1.83	0.6730	93	3727 3933 3969
14.1146	14 17 42.07	+52 26 45.8	21.72	1.28	1.89	0.7437	3	3727 3933 3969 4102
14.1158	14 17 41.85	+52 26 57.4	20.51	1.85	0.90	0.0000	3	2
14.1166	14 17 41.14	+52 30 27.5	22.46	1.42	1.58	1.0151	3	3727 3969 1
14.1177	14 17 40.73	+52 33 51.2	20.82	1.39	6.08	0.7240	3	3727 3969 4102 4340
14.1178	14 17 40.81	+52 30 21.7	22.47	2.19	1.61	···	0	

TABLE 2—*Continued*

CFRS	RA[2000]	δ[2000]	I_{AB}[a]	$(V-I)_{AB}$[b]	Q[c]	z	C[d]	Spectroscopic features[e]
14.1179	14 17 40.83	+52 28 36.4	21.41	1.38	1.84	0.4345	2	3933 3969
14.1189	14 17 40.43	+52 29 49.1	22.12	1.06	2.05	0.7526	3	3727 3969 1
14.1190	14 17 40.48	+52 27 13.8	20.99	1.50	2.81	0.7544	3	3727 3969 4102 4304
14.1193	14 17 40.49	+52 26 19.7	21.48	0.16	4.79	0.0781	4	5007 6562 6725 6300
14.1197	14 17 40.17	+52 32 34.7	21.54	1.04	2.58	0.8240	2	3727 1
14.1200	14 17 40.12	+52 30 16.8	21.93	0.48	2.60	0.2352	2	5007 6562 6725
14.1209	14 17 39.81	+52 29 39.3	20.81	0.39	4.44	0.2342	4	4959 5007 5175 6562 6725
14.1211	14 17 39.64	+52 34 17.7	21.36	0.33	5.25	...	0	
14.1234	14 17 39.29	+52 27 13.0	21.83	2.38	0.95	0.0000	4	2
14.1236	14 17 38.97	+52 30 46.7	19.90	0.68	0.98	0.0000	3	5175 5892 6880
14.1239	14 17 38.96	+52 26 58.0	21.66	0.41	4.02	0.3616	3	3727 4863 4959 5007
14.1241	14 17 38.69	+52 32 50.1	22.50	1.00	2.27	0.9449	8	3727 1
14.1242	14 17 38.79	+52 29 34.6	21.59	0.54	2.48	0.2902	3	3727 5007 1
14.1258	14 17 37.68	+52 29 53.1	22.30	0.97	1.73	0.6449	3	3727 3933 3969 4863 4959 5007
14.1262	14 17 37.52	+52 30 21.2	22.77	0.60	1.57	0.9841	98	3727
14.1266	14 17 37.33	+52 31 09.7	20.83	2.77	0.90	0.0000	4	2
14.1273	14 17 37.40	+52 26 04.2	22.02	0.21	2.75	0.2567	4	3727 4863 4959 5007 6562 6725
14.1275	14 17 37.20	+52 30 41.4	21.51	1.93	2.16	0.7625	2	3727 1
14.1277	14 17 37.21	+52 26 50.3	21.06	1.80	2.38	0.8100	2	3933 3969 4000
14.1289	14 17 36.65	+52 33 23.2	18.13	1.65	1.10	0.0000	4	2
14.1302	14 17 36.12	+52 32 46.8	20.85	0.87	4.17	0.5479	3	3727 3933 3969 4102
14.1303	14 17 35.88	+52 30 29.8	19.97	-0.09	0.95	0.9850	14	2799 3426 3346 3727 3868 3969 4102
14.1311	14 17 35.70	+52 26 45.9	19.98	2.26	4.32	0.8065	3	3885 3933 3969 4304
14.1315	14 17 35.17	+52 33 30.7	20.95	1.56	1.51	0.0000	4	2
14.1316	14 17 35.12	+52 34 35.6	19.53	1.55	4.37	0.4710	3	3933 3969 4000 4102 4304
14.1321	14 17 35.13	+52 25 52.3	21.17	0.32	3.37	0.1058	4	4959 5007 6562 6725
14.1327	14 17 34.79	+52 30 43.1	22.17	0.77	2.83	0.9321	9	3727
14.1329	14 17 34.83	+52 27 52.0	19.52	1.08	3.13	0.3750	3	3727 3969 4102 4304 4863 5175 5892
14.1331	14 17 34.56	+52 33 00.9	22.24	0.95	1.89	0.2590	1	4959 5007 6562
14.1338	14 17 34.29	+52 31 07.0	19.07	0.99	2.29	0.2696	4	3933 3969 4000 4304 4863 5175 5892
14.1346	14 17 33.69	+52 33 49.7	20.95	0.93	2.42	0.5478	4	3727 4959 5007
14.1348	14 17 33.63	+52 34 36.3	20.36	1.78	2.99	0.6130	3	3933 3969 4000 4102 4304
14.1349	14 17 33.89	+52 26 41.7	19.00	2.30	0.93	0.0000	4	2
14.1351	14 17 33.59	+52 31 26.6	20.56	0.93	2.39	0.2357	3	5007 6562 6725
14.1352	14 17 33.56	+52 30 37.6	20.76	1.86	1.03	0.0000	4	2
14.1355	14 17 33.44	+52 29 21.6	21.51	0.80	3.83	0.4801	4	3727 3969 4102
14.1356	14 17 33.49	+52 26 49.2	22.06	1.26	2.94	0.8307	3	3727 3969 4102
14.1368	14 17 32.78	+52 29 38.1	20.92	1.92	3.46	0.7460	92	3933 3969 4000 4102 4304
14.1371	14 17 32.77	+52 27 14.2	18.49	0.14	0.99	0.0000	3	4861 5892 6563
14.1376	14 17 32.32	+52 33 06.5	21.51	0.30	1.82	0.2881	4	3727 4863 4959 5007 6562
14.1385	14 17 32.05	+52 30 42.5	22.39	0.16	2.93	0.3361	3	3727 5007
14.1386	14 17 32.07	+52 29 31.7	21.28	1.05	1.82	0.7413	3	3727 3969 4102
14.1392	14 17 31.58	+52 33 20.9	21.14	1.85	1.63	0.5660	3	4000 4304 1
14.1395	14 17 31.70	+52 26 05.7	21.89	0.85	3.40	0.5301	4	3727 4863 5007
14.1399	14 17 31.38	+52 31 07.3	22.13	0.19	1.80	0.2914	4	4863 4959 5007 6562
14.1419	14 17 30.88	+52 26 44.2	23.07	1.87	1.18	0.2356	93	5007 6562
14.1425	14 17 30.47	+52 30 39.1	22.31	0.28	1.55	0.2090	3	3727 4863 4959 5007 6562
14.1432	14 17 30.15	+52 30 33.3	20.32	0.40	4.24	0.1709	4	3969 4102 4863 4959 5007 6563 6724
14.1436	14 17 29.88	+52 34 13.3	21.15	0.20	3.70	0.2881	4	3727 3969 4304 4863 5007 6562
14.1444	14 17 29.58	+52 31 59.9	22.25	1.63	2.91	0.7422	3	3727 4102 1
14.1446	14 17 29.59	+52 27 59.5	19.99	0.57	2.44	0.3481	4	3727 3885 3969 4102 4340 4863 5007
14.1464	14 17 28.75	+52 27 38.2	21.14	1.85	1.39	0.4620	2	3933 3969 4000 4102 4304
14.1466	14 17 28.50	+52 31 08.7	22.34	1.08	1.48	0.6742	3	3727 3933 3969 4102
14.1467	14 17 28.45	+52 30 38.8	20.91	1.12	4.32	0.6433	4	3727 3969 4102 4863 5007
14.1490	14 17 27.49	+52 33 56.2	21.41	2.32	0.86	0.0000	4	2
14.1491	14 17 27.46	+52 33 09.5	21.75	2.10	2.65	0.6020	1	3727 4000 1
14.1496	14 17 27.54	+52 26 45.3	21.80	1.13	2.03	0.8990	3	3727 3885 3969 4304 4340
14.1502	14 17 27.34	+52 27 32.9	22.49	0.98	2.03	...	0	
14.1503	14 17 27.38	+52 26 09.2	21.98	0.69	1.46	0.3600	3	4863 5007 1
14.1510	14 17 26.71	+52 33 52.9	21.93	1.08	2.49	0.9939	3	3727 3885 3969 1
14.1518	14 17 26.42	+52 29 27.6	20.40	3.32	0.97	0.0000	4	2
14.1525	14 17 26.22	+52 30 31.3	21.61	1.00	3.10	0.7475	4	3727 3885 3969 4102 4340
14.1537	14 17 25.80	+52 27 25.6	22.11	1.89	1.91	...	0	
14.1541	14 17 25.55	+52 30 25.5	22.30	0.96	1.99	0.7427	3	3727 3933 3969 4102 4340
14.1566	14 17 24.57	+52 29 31.3	21.70	0.92	2.31	0.9778	3	2799 3727 3969
14.1567	14 17 24.53	+52 30 25.0	19.79	0.25	1.28	0.4787	14	4102 4340 4863 4959 5007
14.9025	14 17 44.99	+52 28 03.0	18.38	0.77	8.54	0.1550	4	3933 3969 4102 4304 4340 4863 5175 6562
14.9027	14 17 43.03	+52 28 03.5	23.40	0.57	1.56	0.9950	99	3727
14.9301	14 17 35.58	+52 33 32.8	21.01	1.05	2.22	0.5490	3	3727 3969 4102 4304
14.9318	14 17 38.96	+52 33 12.7	20.46	1.55	6.48	0.0000	4	2
14.9705	14 18 21.46	+52 33 12.7	21.27	0.77	3.20	0.6045	3	3727 3969

NOTE.—In any use of these data, attention should be paid to the confidence class that has been assigned to each spectroscopic identification. Identifications with $C \leq 1$ are not used in the CFRS scientific analyses described elsewhere. See CRFS II and this paper for more information.

[a] Measured in isophotal aperture; see CRFS I.

[b] Measured in a 3″ aperture; see CFRS I.

[c] Compactness parameter; see CFRS I.

[d] Confidence class of spectrscopic identification; see CRFS II and this paper.

[e] Features noted in the spectra. These are largely self-explanatory, except that a 1 indicates that the continuum shape supported the identification in cases in which the number of distinct features was small, and 2 indicates the multiple features of an M star.

TABLE 3

SPECTROSCOPIC CATALOG IN THE 2215+00 FIELD

CFRS	RA[2000]	δ[2000]	I_{AB}[a]	$(V-I)_{AB}$[b]	Q[c]	z	C[d]	Spectroscopic features [e]
22.0210	22 18 05.83	+00 14 41.0	20.97	0.33	3.10	0.3300	1	
22.0223	22 18 05.45	+00 18 34.4	20.83	1.77	0.80	0.0000	4	2
22.0240	22 18 04.88	+00 21 30.6	20.66	1.00	1.02	0.0000	4	5175
22.0242	22 18 04.89	+00 18 04.1	22.48	1.45	1.11	0.8631	3	3727 3969 4304
22.0266	22 18 04.40	+00 18 07.3	21.98	1.37	3.17	...	0	
22.0272	22 18 04.12	+00 18 26.0	22.34	1.42	0.73	...	0	
22.0274	22 18 04.06	+00 21 32.6	20.46	0.70	2.94	0.5057	4	3727 3868 4863 4959 5007
22.0285	22 18 03.87	+00 15 06.3	21.46	2.13	3.56	...	0	
22.0288	22 18 03.80	+00 14 49.4	20.20	0.61	0.95	0.0000	4	5175
22.0293	22 18 03.55	+00 21 31.9	22.01	0.75	2.09	0.5420	3	3727 5007
22.0297	22 18 03.58	+00 17 59.4	22.20	1.72	0.73	0.0000	3	2
22.0311	22 18 03.02	+00 21 57.5	21.04	2.00	0.97	0.0000	3	2
22.0321	22 18 02.92	+00 14 28.0	20.93	0.62	3.25	0.4230	2	3727 4000 4304 4959 5007
22.0322	22 18 02.80	+00 18 39.5	21.81	0.91	2.38	0.9160	8	3727 1
22.0323	22 18 02.75	+00 21 29.5	20.81	1.52	3.74	0.0000	1	5892 6880
22.0344	22 18 02.15	+00 17 38.6	21.69	0.93	1.88	0.5195	4	3727 4863 4959 5007
22.0346	22 18 02.05	+00 21 16.1	22.00	3.53	0.87	0.0000	3	2
22.0364	22 18 01.58	+00 15 01.2	21.02	0.86	2.03	0.4296	3	3727 3969 4102 4304 4863 4959 5007
22.0375	22 18 01.26	+00 21 30.9	21.00	1.16	1.59	...	0	
22.0377	22 18 01.19	+00 17 40.6	22.21	1.11	1.33	0.0000	1	5175 6562
22.0378	22 18 01.23	+00 14 24.5	20.34	2.25	0.98	0.0000	3	2
22.0380	22 18 01.19	+00 15 01.7	21.45	1.85	2.35	0.5581	2	3727 3933 3969
22.0383	22 18 01.02	+00 20 50.9	21.83	0.67	3.81	0.2175	2	5007 6562
22.0398	22 18 00.70	+00 17 59.2	22.09	1.53	1.16	1.0731	9	3727
22.0399	22 18 00.55	+00 21 56.2	19.92	1.98	1.86	0.5020	3	3933 3969 4320 1
22.0417	22 18 00.25	+00 21 39.0	22.07	1.07	1.24	0.5943	4	3727 3885 3969 4102 4304 4863
22.0420	22 18 00.30	+00 14 19.5	21.65	1.22	2.83	0.3780	1	4304 5175
22.0429	22 17 59.98	+00 17 54.0	21.95	1.59	1.27	0.6267	4	3727 3969 4102 5007
22.0431	22 17 59.83	+00 21 51.6	20.07	0.35	0.90	0.0000	3	4863
22.0434	22 17 59.80	+00 17 45.9	19.27	0.38	6.27	0.0939	4	4863 5007 6562 6725
22.0443	22 17 59.51	+00 18 26.3	22.16	1.22	0.73	0.0000	1	5175 6562
22.0447	22 17 59.18	+00 14 36.4	22.00	0.04	0.87	0.0000	3	4863 5175 6562
22.0453	22 17 59.04	+00 17 46.0	22.14	1.16	1.21	0.6232	3	3727 4959 5007 1
22.0471	22 17 58.81	+00 14 19.1	21.21	0.79	1.50	...	0	
22.0474	22 17 58.70	+00 21 11.7	21.74	0.64	1.29	0.2812	4	3727 3868 4863 4959 5007 6562 6725
22.0497	22 17 58.39	+00 17 27.5	18.42	1.79	4.63	0.4705	4	3933 3969 4304 1
22.0501	22 17 58.25	+00 18 11.6	20.05	1.80	2.04	0.4243	4	3933 3969 4304 5175
22.0502	22 17 58.26	+00 14 29.8	21.58	0.76	1.44	0.4698	2	3727 1
22.0504	22 17 58.07	+00 21 37.5	21.02	0.88	2.36	0.5379	4	3727 3969 5007 1
22.0510	22 17 57.76	+00 21 54.2	21.44	2.07	0.77	0.0000	4	2
22.0511	22 17 57.83	+00 15 47.8	20.93	1.69	1.22	0.0000	4	2
22.0538	22 17 57.02	+00 21 33.7	22.39	0.87	1.68	...	0	
22.0539	22 17 57.00	+00 20 53.6	19.62	1.17	0.92	0.0000	4	5175
22.0541	22 17 57.01	+00 17 47.3	22.25	2.65	1.86	...	0	
22.0548	22 17 56.67	+00 14 11.5	22.21	2.90	3.46	...	0	
22.0570	22 17 56.10	+00 14 40.8	20.67	2.28	1.12	0.0000	4	2
22.0571	22 17 56.10	+00 14 16.9	22.47	1.18	3.05	0.3980	93	4863 4959 5007
22.0576	22 17 55.92	+00 16 57.9	22.29	0.79	0.93	0.8905	9	3727
22.0577	22 17 55.91	+00 17 48.9	20.04	0.72	0.80	0.0000	4	2
22.0578	22 17 55.79	+00 21 31.9	22.39	0.49	2.13	0.4685	3	3727 4863 4959 5007
22.0579	22 17 55.75	+00 22 07.8	21.71	0.42	1.96	1.1003	9	3727
22.0583	22 17 55.64	+00 18 23.3	21.69	1.47	2.13	0.4312	3	3727 3969 4102
22.0585	22 17 55.60	+00 16 59.2	20.59	1.19	1.86	0.2936	2	4959 5007 6562
22.0599	22 17 55.25	+00 16 57.7	21.74	0.84	1.16	0.8891	9	3727
22.0609	22 17 54.85	+00 17 56.9	20.31	1.91	2.34	0.4750	3	3933 3969
22.0612	22 17 54.75	+00 18 14.7	22.00	2.41	0.71	0.0000	3	2
22.0618	22 17 54.58	+00 17 59.8	22.35	1.44	1.13	0.8300	1	4000
22.0622	22 17 54.58	+00 16 58.7	22.21	0.69	0.91	0.3251	3	3727 3969 5007
22.0631	22 17 54.38	+00 22 06.1	22.29	2.10	0.81	0.0000	3	2
22.0637	22 17 54.01	+00 21 26.7	20.79	1.11	1.93	0.5448	4	3727 4863 5007 3933 3969
22.0641	22 17 53.85	+00 18 07.4	18.21	0.36	0.83	0.0000	3	4863 6562
22.0642	22 17 53.77	+00 22 05.1	19.93	1.42	2.97	0.4650	4	3933 3969 4102 4304 4340 4863
22.0643	22 17 53.81	+00 17 08.3	20.75	0.41	0.71	0.0000	2	6562
22.0661	22 17 53.45	+00 15 12.6	21.25	...	0.96	0.0000	4	2
22.0669	22 17 53.21	+00 14 33.7	20.55	1.21	2.51	0.2920	1	3933 3969 5175
22.0671	22 17 53.03	+00 18 27.6	20.70	0.49	1.89	0.3187	4	3727 3933 3969 4863 4959 5007 6562
22.0674	22 17 52.96	+00 21 57.7	21.77	1.16	0.80	0.0000	4	2
22.0676	22 17 52.93	+00 17 04.8	20.58	0.51	1.74	0.1409	4	4863 4959 5007 6562 6725
22.0683	22 17 52.63	+00 17 56.9	18.91	2.79	0.83	0.0000	4	2
22.0689	22 17 52.51	+00 14 52.0	20.94	1.70	2.27	0.3600	2	3727 4863 5007
22.0693	22 17 52.33	+00 16 45.9	21.52	1.50	1.57	0.5590	2	3727 3969 4304 4340
22.0695	22 17 52.30	+00 14 17.4	19.70	2.34	1.04	0.0000	4	2
22.0708	22 17 51.86	+00 21 11.6	21.25	1.29	4.30	0.7413	94	3727 3969 5007
22.0717	22 17 51.63	+00 21 46.9	19.60	1.21	3.00	0.2794	4	3933 3969 4102 4304 5175 6562
22.0723	22 17 51.48	+00 18 04.8	21.52	0.70	2.36	...	0	
22.0728	22 17 51.37	+00 18 37.1	22.04	1.91	0.73	0.0000	2	2
22.0749	22 17 50.82	+00 17 52.7	19.48	0.83	0.81	0.0000	4	5175 5892 6880
22.0753	22 17 50.75	+00 15 14.4	21.03	0.39	0.88	0.0000	2	5175 6562
22.0758	22 17 50.59	+00 17 00.9	19.03	1.39	2.92	0.2945	3	3933 3969 5175
22.0764	22 17 50.48	+00 17 09.6	22.20	1.29	2.11	0.8194	3	3727 3969
22.0770	22 17 50.21	+00 21 20.1	21.78	1.58	2.36	0.8188	4	3727 3970 4102 4340

TABLE 3—*Continued*

CFRS	RA[2000]	δ[2000]	I_{AB}[a]	$(V-I)_{AB}$[b]	Q[c]	z	C[d]	Spectroscopic features [e]
22.0774	22 17 50.16	+00 20 55.9	21.65	0.95	1.45	0.3280	3	3933 3969 4102 4304
22.0779	22 17 50.05	+00 17 32.0	21.86	1.05	1.35	0.9252	3	3727 3969 4304
22.0789	22 17 49.83	+00 14 17.8	17.84	0.79	0.95	0.0000	3	4863 5175
22.0792	22 17 49.72	+00 18 33.7	22.49	1.73	1.32	0.6546	9	3727 1
22.0795	22 17 49.59	+00 18 08.6	20.69	2.46	0.79	0.0000	4	2
22.0801	22 17 49.38	+00 16 05.7	21.63	0.75	1.42	···	0	
22.0812	22 17 49.13	+00 14 47.9	21.59	1.27	1.26	···	0	
22.0814	22 17 48.90	+00 21 22.2	20.47	1.35	1.69	0.3317	4	3933 3969 4102 4304 5007 5175
22.0819	22 17 48.76	+00 17 18.4	20.85	0.71	2.34	0.2933	4	3727 3868 4863 4959 5007 6562
22.0823	22 17 48.57	+00 21 27.6	18.83	1.49	3.57	0.3315	4	3933 3969 4304 4863 5175
22.0828	22 17 48.48	+00 18 00.5	21.72	1.15	1.25	0.4070	4	3727 3885 4102 4863 4959 5007
22.0832	22 17 48.44	+00 15 15.7	20.15	0.92	1.89	0.2326	4	4863a 6562 6725
22.0843	22 17 48.22	+00 15 08.3	22.10	0.85	2.27	0.9150	9	3727
22.0845	22 17 48.10	+00 21 13.6	20.81	2.15	0.94	0.0000	94	2
22.0847	22 17 48.10	+00 15 09.4	22.93	-0.08	1.46	0.4092	93	3727 4863 4959 5007 1
22.0855	22 17 47.88	+00 16 28.9	20.78	0.56	1.02	0.2100	2	5007 6562 6725
22.0857	22 17 47.76	+00 18 06.3	22.38	9.48	0.87	0.0000	3	2
22.0859	22 17 47.60	+00 21 43.6	21.48	3.01	0.80	0.0000	3	2
22.0861	22 17 47.68	+00 14 41.7	20.58	1.45	0.84	0.0000	4	2
22.0890	22 17 47.05	+00 17 05.1	20.61	1.25	3.76	···	0	
22.0893	22 17 46.95	+00 21 56.8	21.72	0.37	1.38	0.5326	3	3727 3969 4304
22.0902	22 17 46.79	+00 17 56.0	19.49	2.41	1.04	0.0000	4	2
22.0903	22 17 46.76	+00 15 45.1	22.31	0.28	2.53	0.2969	2	3969 4102 4959 5007 6562
22.0910	22 17 46.63	+00 14 53.5	18.57	0.62	1.16	0.0000	4	5175 6562
22.0919	22 17 46.48	+00 16 53.5	21.77	0.43	1.23	0.4738	4	3727 4863 4959 5007
22.0923	22 17 46.30	+00 18 18.9	22.21	1.45	2.83	···	0	
22.0928	22 17 46.24	+00 14 50.5	21.16	1.80	0.91	0.0000	3	2
22.0937	22 17 46.03	+00 14 22.5	21.71	1.33	3.20	···	0	
22.0938	22 17 45.93	+00 21 18.0	18.45	1.19	3.02	0.2510	4	4000 4304 5175
22.0944	22 17 45.83	+00 17 54.9	17.82	1.26	5.74	0.2490	3	3969 4304 5174 5892
22.0945	22 17 45.82	+00 16 54.3	21.89	1.20	2.93	0.6758	3	3727 3933 3969
22.0946	22 17 45.74	+00 21 25.7	19.24	1.17	2.58	0.2500	4	3933 3969 4304 4863a 5175 5892
22.0951	22 17 45.75	+00 15 08.6	21.61	2.00	0.86	0.0000	4	2
22.0953	22 17 45.61	+00 18 18.9	22.27	0.68	2.85	0.9769	8	3727 1
22.0973	22 17 45.14	+00 15 20.5	22.10	0.90	1.96	0.8307	9	3727
22.0975	22 17 45.12	+00 14 47.4	20.21	1.24	2.15	0.4211	3	3727 3969 4102 4304 4863 4959 5007
22.0983	22 17 44.96	+00 14 40.2	22.22	0.70	2.11	0.9997	8	3727
22.0984	22 17 44.96	+00 14 37.5	19.09	1.02	1.01	0.0000	4	5175
22.0988	22 17 44.81	+00 18 29.8	22.76	0.68	2.51	0.4768	93	3727 3969 4863 4959 5007
22.0994	22 17 44.68	+00 17 49.5	19.92	1.65	1.04	0.0000	4	2
22.1001	22 17 44.53	+00 21 22.0	18.91	2.41	1.07	0.4754	4	3727 5007
22.1013	22 17 44.31	+00 15 05.6	20.16	0.65	3.54	0.2306	4	3727 4863 4959 5007 6562 6725
22.1019	22 17 44.19	+00 14 10.7	19.67	0.80	0.93	0.0000	3	2
22.1037	22 17 43.63	+00 17 36.0	21.79	1.78	1.75	0.5500	2	4000
22.1039	22 17 43.60	+00 18 21.1	22.43	1.60	1.08	0.0000	2	2
22.1041	22 17 43.55	+00 21 16.9	20.30	0.23	0.87	0.0000	4	4863 6562
22.1047	22 17 43.42	+00 21 58.4	22.48	0.41	1.12	0.4645	94	3727 4863 4959 5007
22.1064	22 17 43.08	+00 15 08.3	22.08	0.85	1.15	0.5383	3	3727 3868 4863 4959 5007
22.1066	22 17 43.03	+00 14 13.2	18.52	0.57	1.06	0.0000	3	6562
22.1074	22 17 42.86	+00 15 10.2	21.34	0.93	3.47	0.9639	9	3727
22.1078	22 17 42.66	+00 17 43.3	21.93	1.20	1.43	0.6710	1	4000
22.1080	22 17 42.53	+00 21 46.6	22.15	1.27	1.58	0.7550	1	4000
22.1082	22 17 42.49	+00 21 05.1	21.62	0.21	2.25	0.2948	4	3727 4102 4863 4959 5007 6562 6725
22.1084	22 17 42.53	+00 14 21.6	20.29	0.63	4.17	0.2940	3	3727 3969 4959 5007 5175
22.1096	22 17 42.08	+00 13 59.6	22.44	1.74	0.81	0.0000	3	2
22.1097	22 17 42.02	+00 18 46.5	20.56	1.74	1.90	0.5150	4	3727 3933 3969 4304 4863 5175
22.1110	22 17 41.63	+00 22 03.4	20.94	0.38	1.01	0.0000	3	4863 6562
22.1119	22 17 41.46	+00 18 54.8	20.07	1.14	2.85	0.5138	3	3727 3969 4102 4304 4340 5175
22.1121	22 17 41.30	+00 21 30.9	22.26	1.63	1.47	0.6758	4	3727 4863 4959 5007
22.1128	22 17 41.20	+00 14 33.1	21.83	1.31	1.91	0.7535	3	3885 3933 3969 4102
22.1140	22 17 40.83	+00 22 00.1	20.13	2.28	1.06	0.0000	4	2
22.1143	22 17 40.85	+00 17 37.4	20.93	0.23	1.02	0.0000	3	6562
22.1144	22 17 40.75	+00 21 46.3	21.74	0.53	2.27	0.3592	4	3727 3969 4304 4863 4959 5007
22.1153	22 17 40.60	+00 18 21.8	22.42	0.11	1.44	1.3118	9	3727
22.1169	22 17 40.23	+00 17 51.1	21.82	···	0.87	0.0000	4	2
22.1175	22 17 39.99	+00 21 01.3	21.00	0.65	1.61	0.3619	4	3727 4000 4863 4959 5007
22.1181	22 17 39.79	+00 21 45.7	18.73	0.33	0.99	0.0000	2	4863 6562
22.1203	22 17 39.54	+00 15 25.2	21.40	0.88	2.66	0.5360	3	3727 4863 5007
22.1206	22 17 39.46	+00 18 28.8	22.46	0.62	2.39	···	0	
22.1210	22 17 39.30	+00 15 33.0	21.31	0.93	1.60	0.4169	1	3727 3969
22.1220	22 17 38.82	+00 21 19.5	20.75	0.72	2.63	0.3600	4	3727 4000 4304 4863 5007
22.1225	22 17 38.67	+00 18 08.5	22.89	0.27	2.60	0.7373	93	3727 3868 1
22.1227	22 17 38.62	+00 18 07.0	22.84	0.56	1.26	0.7367	93	3727 3969 4863
22.1228	22 17 38.63	+00 15 05.5	21.17	1.41	1.74	0.4150	2	3969 4304 5175
22.1231	22 17 38.42	+00 22 13.3	20.55	0.84	1.84	0.2854	4	3727 3933 3969 4863 5007 6562
22.1232	22 17 38.51	+00 14 44.8	18.15	2.06	1.02	0.0000	4	2
22.1253	22 17 37.80	+00 17 36.9	21.65	2.43	0.98	0.0000	4	2
22.1255	22 17 37.65	+00 18 07.3	20.88	0.47	0.89	0.0000	4	5175
22.1261	22 17 37.52	+00 21 27.7	19.88	2.32	0.99	0.0000	4	2
22.1279	22 17 36.98	+00 18 02.2	21.14	2.05	1.97	0.5940	3	4000 4102 4304
22.1280	22 17 37.01	+00 14 07.3	20.80	1.23	1.50	0.3505	2	3933 3969 4304 5175
22.1294	22 17 36.72	+00 14 25.9	22.09	2.34	1.71	···	0	

TABLE 3—*Continued*

CFRS	RA[2000]	δ[2000]	I_{AB}[a]	$(V-I)_{AB}$[b]	Q[c]	z	C[d]	Spectroscopic features [e]
22.1303	22 17 36.47	+00 18 34.6	19.66	2.45	1.06	0.0000	4	2
22.1309	22 17 36.18	+00 21 24.4	21.54	0.46	1.80	0.2862	4	3727 3969 4863 5007 6562
22.1313	22 17 36.06	+00 17 28.2	21.74	0.84	3.69	0.8191	3	3727 3969
22.1321	22 17 35.86	+00 21 31.0	19.26	1.82	1.00	0.0000	4	2
22.1330	22 17 35.65	+00 18 25.0	20.31	0.54	0.99	0.0000	4	5175
22.1338	22 17 35.42	+00 14 38.6	22.26	0.45	1.84	0.3840	3	3727 5007
22.1339	22 17 35.39	+00 14 34.5	22.06	0.26	1.20	0.3850	4	3727 4863 4959 5007
22.1350	22 17 35.13	+00 14 30.1	22.29	0.53	1.68	0.5111	4	3727 4863 4959 5007
22.1356	22 17 34.96	+00 15 01.0	19.35	1.43	1.96	0.3010	3	3933 3969 5175
22.1362	22 17 34.70	+00 22 00.9	22.16	0.43	2.09	0.3504	3	3727 3969 4959 5007
22.1365	22 17 34.69	+00 17 59.9	19.73	2.29	1.00	0.0000	4	2
22.1368	22 17 34.67	+00 14 31.8	21.76	2.01	0.82	0.0000	3	2
22.1374	22 17 34.48	+00 18 16.2	16.62	0.98	17.66	0.0932	94	3969 4304 4863 5175 5892 6562 6725
22.1395	22 17 34.05	+00 15 11.2	20.75	1.33	1.42	0.3810	3	3933 3969 4304
22.1406	22 17 33.85	+00 18 02.1	22.16	1.16	1.15	0.8182	4	3727 3868 3969 1
22.1409	22 17 33.72	+00 21 33.3	19.97	1.08	1.64	0.2221	3	4000 4304 4863
22.1412	22 17 33.70	+00 14 25.6	18.72	1.53	2.61	0.2980	2	3933 3969 4304 4863a 5175 5892
22.1413	22 17 33.59	+00 21 53.6	22.30	0.39	1.85	0.5440	3	3727 3969 4304 4863 5007
22.1417	22 17 33.57	+00 14 18.6	22.36	0.64	2.84	1.0117	9	3727
22.1433	22 17 33.25	+00 14 32.4	21.59	0.91	1.42	0.3000	2	3969 4102 4303 1
22.1446	22 17 32.91	+00 17 44.6	21.30	2.23	1.04	0.0000	4	2
22.1451	22 17 32.85	+00 14 26.2	19.05	2.54	0.94	0.0000	4	5175
22.1453	22 17 32.75	+00 17 59.6	21.44	1.71	2.85	0.8164	3	3835 3933 3969 4304
22.1455	22 17 32.64	+00 21 46.2	21.66	1.65	0.79	0.0000	4	2
22.1466	22 17 32.53	+00 17 30.0	21.84	1.89	1.70	...	0	
22.1473	22 17 32.28	+00 14 47.7	22.12	1.82	0.79	0.0000	3	2
22.1485	22 17 31.97	+00 14 35.8	20.97	2.51	0.88	0.0000	3	2
22.1486	22 17 31.89	+00 17 59.5	22.28	1.06	1.87	0.9533	8	3727
22.1506	22 17 31.35	+00 14 19.3	20.90	2.46	0.88	0.0000	4	2
22.1507	22 17 31.29	+00 18 24.8	21.44	2.44	1.83	0.8204	3	3933 3969
22.1526	22 17 30.61	+00 18 08.5	20.75	1.94	0.95	0.0000	4	2
22.1528	22 17 30.57	+00 15 28.3	22.17	0.70	3.08	0.6656	3	3727 4863 4959 5007
22.1529	22 17 30.47	+00 21 11.8	22.02	0.41	0.97	...	0	
22.1533	22 17 30.52	+00 14 46.9	22.23	1.70	1.65	...	0	
22.1538	22 17 30.34	+00 14 36.1	22.40	2.53	1.01	0.0000	2	2

NOTE.—In any use of these data, attention should be paid to the confidence class that has been assigned to each spectroscopic identification. Identifications with $C \leq 1$ are not used in the CFRS scientific analyses described elsewhere. See CRFS II and this paper for more information.

[a] Measured in isophotal aperture; see CRFS I.

[b] Measured in a 3″ aperture; see CFRS I.

[c] Compactness parameter; see CFRS I.

[d] Confidence class of spectrscopic identification; see CRFS II and this paper.

[e] Features noted in the spectra. These are largely self-explanatory, except that a 1 indicates that the continuum shape supported the identification in cases in which the number of distinct features was small, and 2 indicates the multiple features of an M star.

final review of all 1010 CFRS spectra (by S. J. L.) after the completion of the threefold comparisons of independent reductions described in CFRS II. Since only one other object (in the 0000+00 field) in the 1010 spectra in the CFRS appears to have been misclassified in this way, we have simply altered the entries in Table 2 for these two objects.

In the 2215+00 field, there are 189 objects in the statistically complete sample plus an additional 10 objects in the supplementary catalog. The photometric catalog in the area surveyed spectroscopically contains 731 objects, so the statistically complete sample represents a sampling rate of 26%. There are 29 spectroscopically unidentified objects, and the spectroscopic identification rate is thus 85%. The stellar fraction in this relatively low latitude field is 35%, and this largely accounts for the 30% higher surface density of objects in the photometric catalog of this field relative to the 1415+52 field described above. The redshift distribution in this field is shown in Figure 10.

The 2215+00 field contains the SSA-22 field described by Lilly, Cowie, & Gardner (1991). It and the surrounding areas have also been extensively studied by the Hawaii group, allowing some external checks on our spectroscopic identifications.

5. COMPARISON WITH SPECTROSCOPIC IDENTIFICATIONS BY THE HAWAII GROUP

Unfortunately, excluding objects previously published byLilly et al. (1991) and Lilly (1993), there are only eight objects in common between the CFRS sample and that of Songaila et al. (1995). As shown in Table 4, the identifications

TABLE 4

COMPARISON OF SPECTROSCOPY WITH SONGAILA ET AL. IN THE 2215+00 FIELD

CFRS			HDS	
Identification	z	Class	Identification	z
22.1210	0.417	1	265	0.304
22.1228	0.415	2	239	...
22.1280	0.351	2	231	0.348
22.1294	...	0	251	0.822
22.1339	0.385	4	280	0.384
22.1350	0.511	4	283	0.513
22.1417	1.012	9	259	1.010:
22.1433	0.300	2	273	0.303

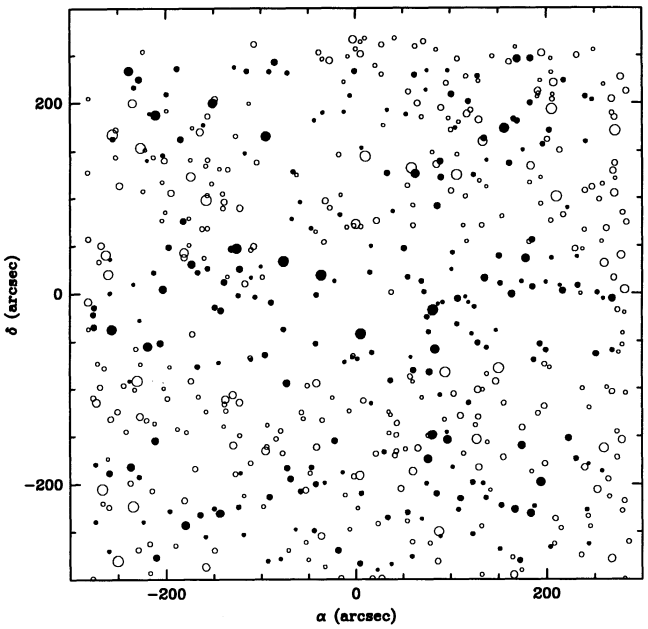

FIG. 7.—The 1415+52 field showing objects observed spectroscopically (*filled symbols*) with other objects with $I_{AB} < 22.5$ marked as open symbols. The symbol size represents the isophotal magnitudes of the objects. The positions are relative to the field center $14^h17^m53^s.73$, 52°30′31″. North is at the top, and east is to the left.

agree in five cases with mean and r.m.s. redshift differences of 0.0002 and 0.0023, respectively. The r.m.s. is similar to that found above. For two of the sources one or the other group did not identify the object. For the eighth source, although the identifications disagree, they are both insecure identifications (confidence class 1 in the CFRS, a class that we have not

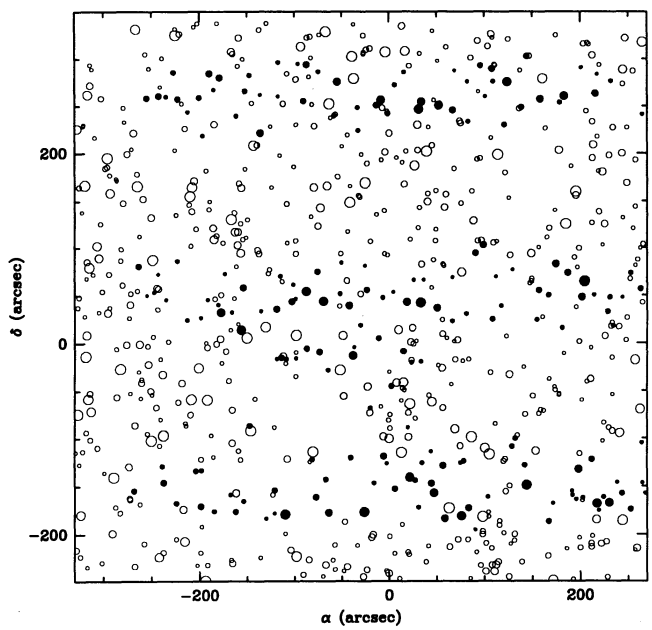

FIG. 8.—The 2215+00 field showing objects observed spectroscopically (*filled symbols*) with other objects with $I_{AB} < 22.5$ marked as open symbols. The symbol size represents the isophotal magnitudes of the objects. The positions are relative to the field center $22^h17^m48^s.0$, +00°17′34″. North is at the top, and east is to the left.

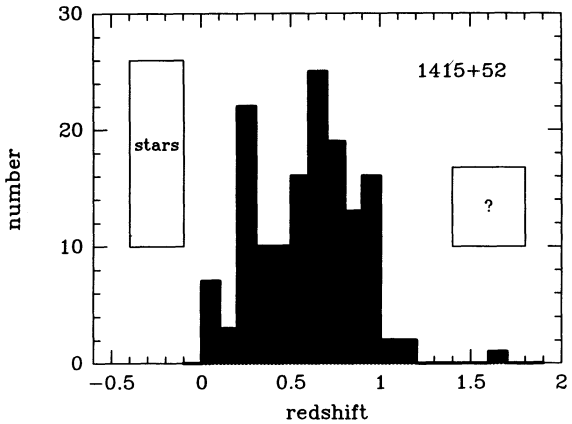

FIG. 9.—Redshift distribution for galaxies in the 1415+52 field. Boxes represent relative numbers of stars and unidentified objects (confidence class 0 or 1).

regarded as a "usable" redshift determination and ":" in Songaila et al. 1995).

6. CONCLUSIONS

We have investigated whether the curvature of the continuum in the neighborhood of the emission line can be used to identify the emission line in objects in which a single isolated emission line is the distinguishing spectroscopic feature, especially for objects with $\lambda_{em} > 6560$ Å, where there is potential ambiguity between [O II] λ3727 at $z > 0.76$ and Hα at low redshift. We find a clear separation on a two-parameter plot between objects in which the identification of the line is secure on the basis of other features. Applying this method to the 35 single emission-line galaxies with $6560 < \lambda < 7520$, we find that in at least 85% (and up to 100%) of these galaxies the line should be identified with [O II] λ3727. We argue that this most likely applies also for galaxies in which the line is at $\lambda_{em} > 7520$ Å, where we are unable to adequately sample the continuum.

We have also studied the statistics of the independent identifications of objects that were observed on more than one occasion. The independent identifications of objects that were identified more than once can be used to test or calibrate empirically the confidence classes that we have used in the CFRS to describe the reliability of the spectroscopic identifica-

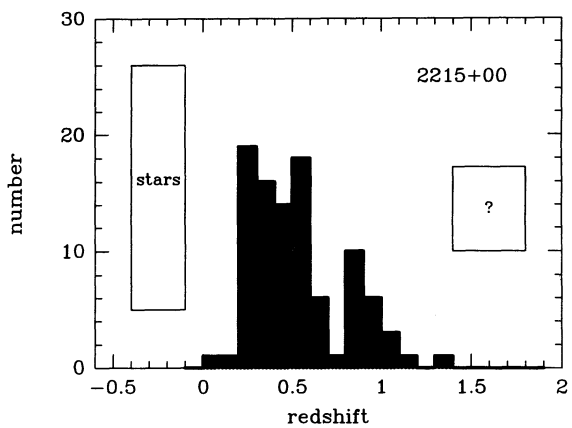

FIG. 10.—Redshift distribution for galaxies in the 2215+00 field. Boxes represent relative numbers of stars and unidentified objects (confidence class 0 or 1).

tions. We find good agreement between the success rates and the initial definition of each confidence class. In addition, we find that repeated observations are frequently (70%) able to secure an identification for an object that was initially unidentified after one observation. This implies that many of the objects in the survey that have not been identified could be identified if they were reobserved.

We thank Gabriela Mallen-Ornelas for her assistance with the computations of the GISSEL spectra. We also thank the Directors of CFHT and our respective national TACs for their support of the CFRS project, and the referee for his careful reading of the text. S. J. L.'s research is supported by NSERC of Canada and the project has been facilitated by a travel grant from NATO.

REFERENCES

Bruzual A., G., & Charlot, S. 1993, ApJ, 405, 538
Crampton, D., Le Fèvre, O., Lilly, S. J., & Hammer, F. 1995, ApJ, 455, 96 (CFRS V)
Fomalont, E. B., Windhorst, R. A., Kristian, J. A., & Kellerman, K. I. 1991, AJ, 102, 1258
Hamilton, D. 1985, ApJ, 297, 371
Hammer, F., Crampton, D., Lilly, S. J., Le Fèvre, O., & Kenet, T. 1995b, MNRAS, submitted (CFRS VII)
Le Fèvre, O., Crampton, D., Hammer, F., Lilly, S., & Tresse, L. 1994, ApJ, 423, L89
Le Fèvre, O., Crampton, D., Lilly, S. J., Hammer, F., & Tresse, L. 1995a, ApJ, 455, 60 (CFRS II)
Lilly, S. J. 1993, ApJ, 411, 501
Lilly, S. J., Cowie, L. L., & Gardner, J. P. 1991, ApJ, 369, 79
Lilly, S. J., Le Fèvre, O., Crampton, D., Hammer, F., & Tresse, L. 1995, ApJ, 455, 50 (CFRS I)
Songaila, A., Cowie, L. L., Hu, E. M., & Gardner, J. P. 1995, ApJS, 94, 461